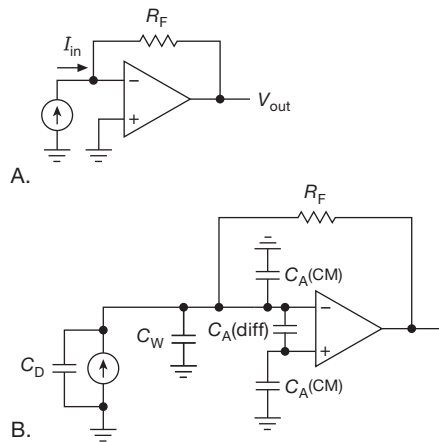


### 4x.3 Transresistance Amplifiers

We introduced the basic current-to-voltage, or *transresistance*, amplifier configuration in §4.3.1: an op-amp with feedback resistor  $R_f$  converts an input current  $I_{in}$  at the summing junction to an output voltage  $V_{out} = -R_f I_{in}$ . It is called transresistance because its “gain” (output/input) has units of resistance:  $\text{Gain} = V_{out}/I_{in} = R_f$ . (You often see the term “transimpedance” and “TIA” used instead, perhaps suggesting that you ought to be worrying about more general feedback circuits, and phase shifts; but in the real world people design these things as simple current-to-voltage amplifiers, and so we often say “transresistance amplifier,” or “current-to-voltage amplifier.”)



**Figure 4x.16.** Transresistance amplifiers. A. Basic circuit. B. Including real-world parasitic input capacitances.

#### 4x.3.1 Stability problem

The basic transresistance amplifier is shown again in Figure 4x.16A, and with real-world complications in Figure 4x.16B. The problem with the simple circuit is, simply, that it will probably oscillate! That’s because photodiodes (and other detectors, or current-output devices in general) have some intrinsic capacitance  $C_D$ , and this capacitance at the input forms a lowpass filter with  $R_f$  (with  $-3\text{ dB}$  “breakpoint”  $f_{RCin} = 1/2\pi R_f C_D$ ), hence a lagging phase shift that approaches  $-90^\circ$  well beyond  $f_{RCin}$ . That’s often well below the op-amp’s gain–bandwidth product  $f_T$ ,

so the effect is to add nearly  $90^\circ$  of lagging phase shift to the feedback path, augmenting the op-amp’s  $90^\circ$  (or greater) lagging internal phase shift. The situation is shown in the Bode plot of Figure 4x.17, where the feedback network contributes a second pole that increases the roll-off to  $12\text{ dB/octave}$ , and the phase shift to  $-180^\circ$ , at a frequency where the loop gain is still greater than unity; and it crosses the unity gain axis with still greater slope. That’s the prescription for oscillation.

Note, by the way, the additional capacitances from the summing junction to ground shown in Figure 4x.16B: the op-amp’s input capacitance (both differential and common-mode), and wiring capacitance. For the purposes of circuit behavior, they’re all in parallel:  $C_{in} = C_D + C_A + C_W$ . Which capacitance dominates the sum depends on the size of the detector, the op-amp’s internal input circuit, and the wiring. With a fast, small-geometry detector, the op-amp’s input capacitance may well dominate; whereas a large-area detector’s capacitance is likely to dominate (unless significant lengths of shielded cable are used with a remote detector). As we’ll see shortly, the more capacitance you have, the poorer the performance (in terms of speed and noise). So it’s always best to avoid adding significant capacitance, where possible. For example, if your detector is some distance from the rest of your circuit, it is often a good idea to put the transresistance preamp right at the detector, bringing the amplified voltage output back through shielded cable; this also has the advantage of minimizing noise pickup on the low-level, high-impedance input signal via capacitive and inductive pickup, ground loops, and the like. Also, detector capacitance decreases markedly with increasing applied back-bias, so speed is improved (but leakage current is introduced) by returning the detector common terminal to a quiet (i.e., well bypassed) bias supply instead of ground (Figure 4x.18).

#### 4x.3.2 Stability solution

The simplest solution to this problem is to put a small parallel compensation capacitance  $C_f$  across the feedback resistor, as in Figure 4x.19. It’s easiest to understand what’s going on with a Bode plot (Figure 4x.17).  $C_f$  stops the  $6\text{ dB/octave}$  roll-off of the feedback network at frequency  $f_c = 1/2\pi R_f C_f$  (that’s where the magnitude of  $C_f$ ’s reactance equals  $R_f$ , and is roughly the roll-off response frequency of the amplifier), which makes the overall roll-off of loop gain revert to its original  $6\text{ dB/octave}$  slope (and corresponding  $90^\circ$  lagging phase shift). (In official jargon this is known as putting a “zero” into the feedback network.) The trick is to choose  $C_f$  so that the resulting closed-

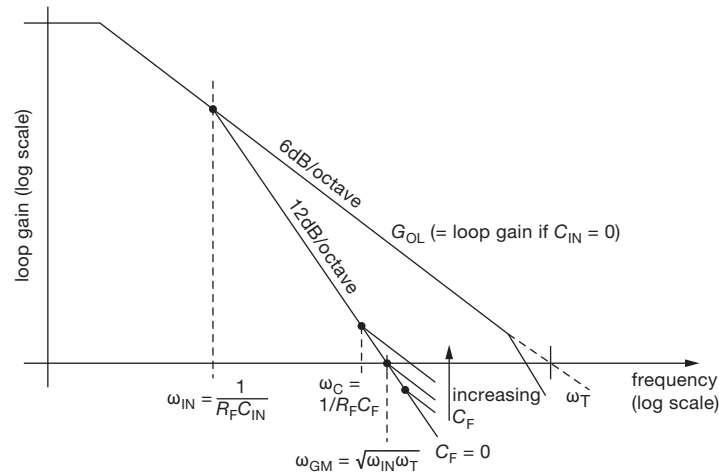


**Figure 4x.17.** Bode plot (log magnitude of gain vs log frequency for the transresistance amplifier). For stability the closed-loop gain curve must intercept the unity-gain axis at a 6 dB/octave slope.

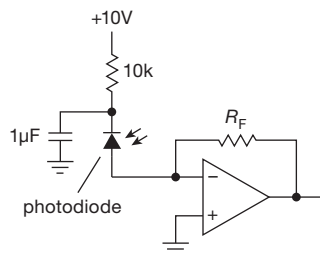


**Figure 4x.18.** Reverse biasing a photodiode decreases capacitance and increases speed (but at the expense of “dark current”). Be sure to use a clean, bypassed bias supply; choose the series resistor so that the drop across it is small compared with the bias voltage, at the maximum anticipated photodiode current.

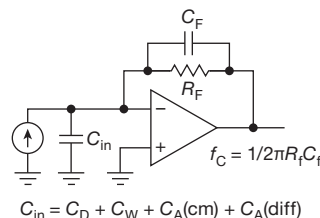


**Figure 4x.19.** Transresistance amplifier with stabilizing feedback capacitor  $C_F$ .

loop gain plot (Figure 4x.17) has reverted safely back to 6 dB/octave somewhat before reaching the unity gain axis.

Here’s how you do it: First note that the unstabilized amplifier has the loop gain crossing the axis halfway (logarith-

mically) between  $f_{RCin}$  and  $f_T$ ; that is, at a frequency<sup>9</sup> that is the geometric mean:

$$f_{GM} = \sqrt{f_{RCin} f_T}. \quad (4x.1)$$

If we were to choose  $C_f$  so as to put  $f_c$  at that frequency, we would be living dangerously – the loop gain plot would be in the midst of reverting to 6 dB/octave as it crossed the unity gain axis; to state things more accurately, the phase shift of the feedback network would have dropped to 45°, as  $RC$  circuits always do at their 3 dB points. The result would be an amplifier that is probably stable in the sense of not oscillating, but it might exhibit overshoot and ringing following a transient; and its closed-loop frequency response would exhibit “peaking,” specifically a bump of about 1.3 dB near the unity-gain crossing frequency  $f_{GM}$  (we’ll call this response trace  $f_a$ ).

So, we choose  $C_f$  a bit larger. A common procedure is to choose  $C_f$  so that  $f_c = 1/2\pi R_f C_f = \sqrt{f_{RCin} f_T/2}$ , i.e., at about 70% of the geometric mean. This generally ensures good stability, and produces a closed-loop response that is maximally flat (actually, a second order Butterworth, see Chapter 6), without any peaking, and is down 3 dB at  $f_{GM}$  (Figure 4x.20). You’ll often see a parameter called the “damping ratio,” with the symbol  $\zeta$  (zeta). The choice

$$f_c = 0.7 f_{GM} \quad (4x.2)$$

<sup>9</sup> An op-amp’s  $f_T$  is the extrapolated frequency at which the log-log curve of open-loop gain versus frequency crosses the unity gain axis, extended from a lower frequency where there is plenty of gain and where the slope is 6 dB/octave (i.e.,  $\propto 1/f$ ). On datasheets this is usually called the gain-bandwidth product, GBW.

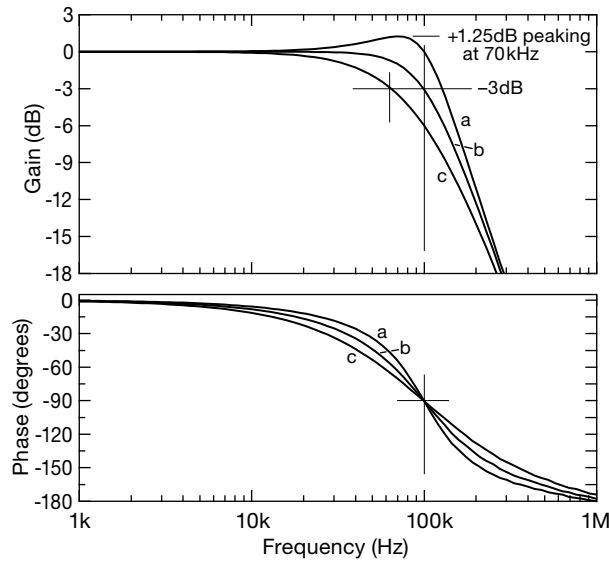


**Figure 4x.20.** TIA frequency response (normalized transresistance gain and phase vs frequency) for three choices of  $C_f$ , namely those corresponding to characteristic frequencies  $f_c = 0.7f_{GM}/\zeta$ , with the damping ratio  $\zeta$  equal to (a) 0.7, underdamped, (b) 1.0, critically damped, and (c) 1.4, overdamped. This SPICE-modeled transimpedance amplifier's bandwidth is 100 kHz; the convergence in gain at high frequencies is controlled by the op-amp, with a slope of 12 dB/octave.

corresponds to a damping ratio  $\zeta = 1$ .

If  $C_f$  is chosen still larger, it produces an overall amplifier bandwidth at a lower frequency (which we'll call  $f_b$ ) equal to the roll-off frequency of the  $RC$ , i.e.,  $f_b = f_c = 1/2\pi R_f C_f$ ; the corresponding frequency response exhibits the usual slow roll-off characteristic of a single  $RC$  lowpass (a single “on-axis pole,” Figure 1.104), with the familiar  $RC$  step response (Figure 1.34). But if  $C_f$  is chosen for maximally flat response (i.e.,  $f_c = 0.7f_{GM}$ ), the result is to introduce just the right amount of “peaking” to extend the amplifier's response to  $f_b = f_{GM}$ , and to speed the step response so it smartly moves to the new output voltage with minimal overshoot (Curve b of the SPICE results in Figures 4x.20 and 4x.21, and seen in the measured  $C_f = 2.4$  pF waveform of Figure 4x.26).<sup>10</sup>

It's customary to define the bandwidth of an amplifier by measuring the frequency at which the gain has fallen by 3 dB. But this simple measure does not take into account the possibility of overdamping, gain peaking due to underdamping, etc. The figure shows that an underdamped

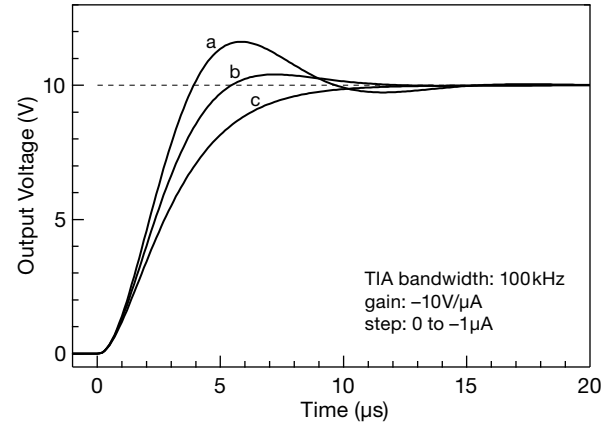


**Figure 4x.21.** TIA step response for the same three choices of  $C_f$  as in Fig. 4x.20.

amplifier appears to have more bandwidth. One useful approach to determining bandwidth is to measure the frequency at which the phase shift reaches  $-45^\circ$ . This is particularly relevant if the amplifier is used inside a feedback loop, e.g., in a scanning tunneling microscope preamp (see §8.11.12). Measured in this way,<sup>11</sup> an underdamped amplifier has more bandwidth, and an overdamped amplifier has less. As an example, here are SPICE results for the  $-3$  dB and  $-45^\circ$  frequencies of a sample TIA with  $f_c = 100$  kHz:

	damping, $\zeta$	$f_{-3\text{dB}}$	$f_{-45^\circ}$
a	0.7	129 kHz	62.7 kHz
b	1.0	100 kHz	51.5 kHz
c	1.4	66 kHz	40.8 kHz

### 4x.3.3 An example: PIN diode amplifier

As an example, let's design a photodiode amplifier for use with a typical silicon PIN diode of  $5\text{ mm}^2$  active area. These popular devices come in a TO-5 transistor package with glass window, and are meant to be operated with a back bias of 10 V to 20 V. Examples are the S1223 from Hamamatsu and the PIN-5D from UDT, with closely similar characteristics: terminal capacitance  $C_D = 10$  pF at 20 V back bias, cutoff frequency (3 dB down)  $f_c = 30$  MHz (corresponding to a rise time  $t_r \approx 0.35/f_c = 12$  ns), and a red-weighted visible-light response rising to a maximum close to  $1\text{ }\mu\text{m}$  wavelength.

A comment on detector speed: The rise time specification tells you the “datasheet speed” of the detector (usually specified for some wavelength of incident light, and with

<sup>10</sup> In the language of “root locus” in the  $s$ -plane, one would say that a single on-axis dominant pole has morphed into a pair of off-axis poles.

<sup>11</sup> That is, ignoring other aspects such as settling time, ringing, and the like.

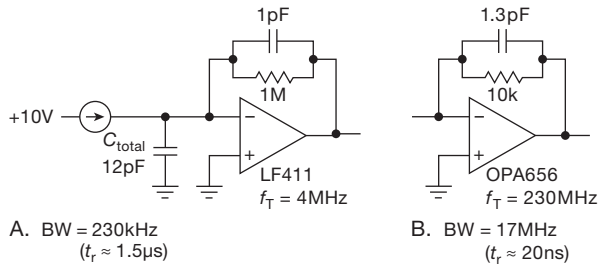


**Figure 4x.22.** Photodiode amplifier examples. A. Using jellybean LF411 ( $f_T=4\text{ MHz}$ ), with  $G=1\text{ V}/\mu\text{A}$ . B. Using wideband OPA656 ( $f_T=230\text{ MHz}$ ), with  $G=10\text{ mV}/\mu\text{A}$ .

some standard load resistance, usually  $50\Omega$ ); it depends on the detector's capacitance (which forms an  $RC$  time constant with the load resistance), and also upon the physics of charge carrier transit time in the detector itself (which in turn depends on semiconductor properties, junction geometry, and applied bias voltage). Depending upon your circuit, you may or may not achieve that “ $50\Omega$ -load” detector speed.<sup>12</sup> As we'll see, achieving adequate bandwidth may be harder than you think!

Let's arbitrarily choose the transresistance gain ( $V_{\text{out}}/I_{\text{in}}$ ) to be  $1\text{ M}\Omega$ ; that becomes the value of the feedback resistor:  $R_f=1\text{ M}\Omega$ . We'll see shortly that this is not a wise choice, if we care about speed. For the op-amp let's start with our standard jellybean LF411, with a gain-bandwidth product  $f_T=4\text{ MHz}$  (typ). The amplifier datasheet gives no information about input capacitance, but it's probably safe to guess a value of about  $C_A=2\text{ pF}$ , giving a total input capacitance  $C_{\text{in}}=C_D+C_A=12\text{ pF}$ . In combination with the  $1\text{ M}\Omega$  feedback resistor, this produces a roll-off beginning at  $f_{RC\text{in}}=13\text{ kHz}$ .

Next we calculate the value of feedback capacitor  $C_f$  to ensure stable operation. The geometric mean of  $f_{RC\text{in}}$  and  $f_T$  is  $f_{GM}=2.3\times 10^5\text{ Hz}$ . For optimum transient performance and good stability, we now choose  $C_f$  so that its characteristic frequency, in combination with the existing  $R_f$ , is 70% of that value:  $1/2\pi R_f C_f=0.7f_{GM}$ , giving  $C_f=1.0\text{ pF}$ . The resulting amplifier has a 3 dB bandwidth of  $f_b=230\text{ kHz}$ , (equal to  $f_{GM}$ ), and a rise time of approximately  $t_r\approx 0.35/f_b=1.5\mu\text{s}$ . (Figure 4x.22A)

### A. Gaining speed

Our amplifier's bandwidth is only 1% of the detector's datasheet speed! And we got only 230kHz response, even

though we used a 4 MHz op-amp. What's going on here? There are two problems, actually: The large feedback resistor formed a very low frequency roll-off (at 13 kHz) with the input capacitance; and the final bandwidth is the geometric mean of that with op-amp's modest  $f_T$ .

Let's try a faster amplifier: The low-noise JFET-input OPA627 (a JFET version of the popular low-noise bipolar OP-27) has an  $f_T$  of 16 MHz, which sounds like it should help. However, it also has a total input capacitance of  $C_A=15\text{ pF}$  (the sum of 8 pF of differential input capacitance and 7 pF of common-mode input capacitance), which pushes the input roll-off down to 6.4 kHz.<sup>13</sup> If you go through the design procedure as above, you'll find that  $C_f=0.7\text{ pF}$ , and the 3 dB bandwidth of the completed amplifier is  $f_b=f_{GM}=320\text{ kHz}$ , a minor improvement over our first design.

We can improve things by using an OPA637, which is a decompensated OPA627 ( $G_{\text{min}}=5$ ). Note an important fact: it's not necessary to use unity-gain compensated op-amps in a transresistance configuration if the op-amp's second breakpoint (its “second pole,” the frequency at which its open-loop gain begins dropping at 12 dB/octave) is well above  $f_c$ . The OPA637's  $f_T$  of 80 MHz allows us to extend  $f_c$  from 320 kHz to a more respectable 715 kHz. But we're still suffering from the penalty of the op-amp's high input capacitance.

### B. “Pedal to the metal”

OK, let's really step on the gas: The high-speed JFET-input OPA656 has an  $f_T$  of 230 MHz, and total input capacitance of  $C_A=3.5\text{ pF}$ . Going through the same design procedure, you'll find that  $f_{RC\text{in}}$  is still 13 kHz (as with the LF411), but the completed amplifier's bandwidth is now  $f_b=1.7\text{ MHz}$  (with a smaller value of feedback capacitance  $C_f=0.13\text{ pF}$  – see comments below). This is almost an order of magnitude better speed than our first pathetic attempt (because the op-amp's  $f_T$  is nearly 2 orders of magnitude higher); but it's still more than an order of magnitude slower than the detector itself (recall  $f_c=30\text{ MHz}$ ). We can do somewhat better here by using a decompensated op-amp (an OPA657,  $f_T=1.6\text{ GHz}$ ,  $G_{\text{min}}=7$ ), which pushes  $f_b$  up to a more respectable 4 MHz. We can't go much further down the path of increasing  $f_T$ , certainly not the factor of several hundred that we evidently still need.

One reasonable solution, if full speed is needed, is to trade off noise performance for speed, by reducing the gain

<sup>12</sup> However (looking on the bright side) you may in fact be able to do better (e.g., when the detector is loaded into the low-impedance presented by a good TIA, or when it is bootstrapped).

<sup>13</sup> The higher capacitance is related to the op-amp's lower  $e_n$  specification,  $4.5\text{ nV}/\sqrt{\text{Hz}}$  versus  $25\text{ nV}/\sqrt{\text{Hz}}$ ; we'll see the important significance of that later.

of the transresistance stage, then follow it with a wideband voltage amplifier. For example, if we reduce the feedback resistor to  $R_f = 10\text{ k}\Omega$  (gain of  $10\text{ V/mA}$ ), we drive the input pole up by a factor of 100, to  $f_{RCin} = 1.3\text{ MHz}$ . The completed amplifier's resulting bandwidth goes up by the square root of that factor, or a factor of 10, to  $f_b = 17\text{ MHz}$ ; the corresponding value for  $C_f$  is  $1.3\text{ pF}$ . With this design we are getting most of the detector's speed (and we could do still better with the decompensated OPA657). Whether we can accept the lower gain depends on issues of noise, which are discussed in Chapter 8 (§8.11).

Another interesting solution is to *bootstrap* the detector, greatly reducing the effective input capacitance seen at the TIA's input; we illustrate this important technique in §4x.3.4.

### C. Sub-picofarad capacitors

The calculated value of feedback capacitance in our last iteration –  $C_f = 0.13\text{ pF}$  – sounds awfully small; can you actually get such capacitors? That's an interesting question, but you might ask first how much “parasitic” capacitance there is between the leads of the feedback resistor itself. We treat this and similar topics in Chapter 1x (properties of components); we have found, by actual measurement, that a standard metal-film resistor (“RN55D-type”) has something like  $0.07\text{ pF}$  –  $0.15\text{ pF}$  of parasitic parallel capacitance, the exact value depending on manufacturer and resistance value. So, you might need to add a tiny bit of capacitance across the resistor, perhaps using a “gimmick,” the official term for a pair of short insulated wires that you twist up until there's enough capacitance. When dealing with circuits like this, in which a fraction of a picofarad has important effects, be careful about component placement and lead dress; for example, the feedback resistor (and perhaps the inverting input pin of the op-amp) should be raised up from the circuit board to minimize capacitance to ground and to other signals. You often see similar advice when dealing with ultra-low input currents (femtoamps), namely to float the input leads, or support them on a Teflon standoff insulator.

What should you do if the calculated feedback capacitance comes out *less* than the parasitic capacitance of the feedback resistor? One solution is to reduce the feedback resistor value until the calculated capacitance is about equal to the parasitic capacitance. This reduces the transresistance gain of the amplifier, of course, perhaps requiring additional gain downstream.<sup>14</sup> A clever alternative is

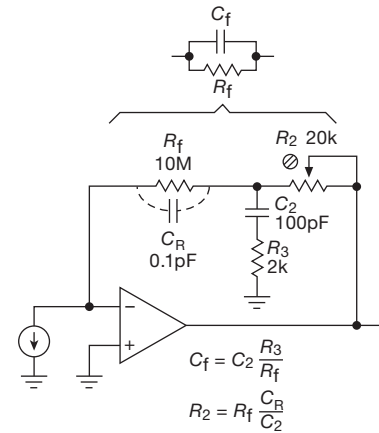


**Figure 4x.23.** “Pole-zero” trick when the parasitic capacitance  $C_R$  of the gain-setting feedback resistor  $R_f$  is itself larger than the calculated shunt feedback capacitance.

shown in Figure 4x.23: Here the unavoidable time constant  $R_f C_R$  of the feedback resistor with its own parasitic capacitance  $C_R$  (a “zero”) is canceled by a deliberate lagging time constant  $R_2 C_2$  (a “pole”); then the addition of a resistor  $R_3$  reintroduces a zero with time constant  $C_2 R_3$ . For example, if a certain circuit needed  $C_f = 0.02\text{ pF}$  across a  $10\text{ M}\Omega$  feedback resistor, we would be in trouble because of the  $\sim 0.1\text{ pF}$  of parasitic capacitance. We cancel this by choosing  $R_2 = 10\text{ k}$  and  $C_2 = 100\text{ pF}$ ; then we choose  $R_3 = 2\text{ k}$ , as shown.<sup>15</sup> We haven’t seen this trick described elsewhere, but we’ve used it successfully in several wideband photodiode amplifiers.

Figure 4x.24 shows another trick, helpful when dealing with these small-value compensation capacitors. Here the effective feedback capacitance is the fraction of  $C_f$  set by trimmer  $R_1$ .

To recapitulate the major results: The “bandwidth” of this properly stabilized current-to-voltage amplifier is far less than the op-amp’s gain–bandwidth product  $f_T$ . It is, rather, at the geometric mean of that frequency and the (much lower) characteristic frequency set by the time constant of the total input capacitance and the feedback resistor. This shows why input capacitance compromises speed,

<sup>14</sup> It also increases  $R_f$ ’s Johnson noise contribution – see the extensive discussion in Chapter 8 (§8.11).

<sup>15</sup> That is,  $R_3 C_2 = R_f C_f$ , where  $C_f$  was the desired feedback capacitance ( $0.2\text{ pF}$ ) appropriate to the gain-setting feedback resistance  $R_f$  ( $10\text{ M}\Omega$ ). Note how the new effective  $C_f$  is well predicted, set by low-tolerance parts.  $R_2$  has to be adjustable, because we don’t know the value of the stray capacitance  $C_R$ ; it should be adjusted for a flat gain response in the crossover region,  $f = 1/2\pi R_f C_R$ , about  $160\text{ kHz}$  in this case, well below the circuit’s  $f_{3dB}$  bandwidth. Choosing a  $20\text{ k}$  trimmer for  $R_2$  allows canceling  $0\text{ pF}$  to  $0.2\text{ pF}$  of stray capacitance  $C_R$ .



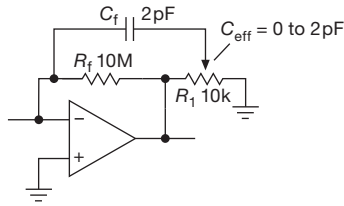


**Figure 4x.24.** Creating a “tunable” low-value feedback capacitor. The total effective feedback capacitance includes  $\sim 0.1$  pF of stray capacitance of  $R_f$  (not shown).

and the surprising need for op-amps that are much faster than you might have guessed. And we’ll see presently how input capacitance also degrades noise performance (we saw it initially in Chapter 8 of AoE3 (§8.11.3)).

#### 4x.3.4 A complete photodiode amplifier design

The circuit of Figure 4x.25 should help tie these ideas together.<sup>16</sup> It’s the basic design of RIS-617, a photodiode amplifier that has been in wide use in the laboratories at our Rowland Institute. For the transimpedance stage we chose the JFET-input OPA637 (or equivalent ADA4637) for its combination of low input current and low noise voltage ( $e_n = 4.5$  nV/ $\sqrt{\text{Hz}}$ ), combined with wide bandwidth ( $f_T = 80$  MHz). This op-amp is the decompensated ( $G > 5$ ) version of the unity-gain-stable OPA627 (which has  $f_T = 16$  MHz); it’s suitable for a transimpedance application like this, owing to the aggressive compensation provided by the external compensation capacitor  $C_f$ . And of course that extra bandwidth translates into improved amplifier speed.

Less obvious is the desirability of low op-amp input noise voltage,  $e_n$ . At first sight it might seem to be of little concern, perhaps contributing only that quantity of noise voltage at the output. That would be wrong. In fact, as we saw in Chapter 8, the op-amp’s  $e_n$  grinds up against the input capacitance  $C_{in}$  to create an effective input noise current  $i_n = e_n \omega C_{in}$  (which we like to call “ $e_n C$ ” noise). This can easily dominate over all other sources of noise, particularly when you’re striving for substantial bandwidth.

In this circuit we chose  $R_f$  for a modest first-stage transimpedance gain ( $0.1$  V/ $\mu\text{A}$ ), with a second stage of selectable voltage gain to set the overall instrument gain. The trade-off is speed (smaller  $R_f$ , thus greater  $f_{RCin}$ ) versus noise (larger  $R_f$ , thus less Johnson noise current  $i_n = \sqrt{4kT/R_f}$ ; see §8.11).

In a transimpedance amplifier input capacitance is the

villain: it drives down the bandwidth (via necessarily larger  $C_f$ ), and it drives up the noise (via the input  $i_n$  produced by the op-amp’s  $e_n$  imposed across  $C_{in}$ ). Because high-performance transimpedance amplifiers are generally expected to work properly with rather large input capacitances<sup>17</sup> (up to 1000 pF), we added a 2-stage bootstrap follower ( $Q_1 Q_2$ ), which reduces the effective input capacitance at signal frequencies by roughly a factor of ten (thus 100 pF maximum).  $Q_2$  is a very low noise ( $0.8$  nV/ $\sqrt{\text{Hz}}$ ) JFET<sup>18</sup> of high transconductance ( $\sim 25$  mS, thus  $\sim 40 \Omega$  output impedance), here buffered by  $Q_1$  for plenty of drive muscle. See §8.11 for more detail.

To figure the compensation capacitor  $C_f$ , we take the maximum effective  $C_{in} = 100$  pF, for which  $f_{RCin} = 16$  kHz,  $f_c = 1.1$  MHz, and critical damping ( $\zeta = 1$ ) would require  $C_f = 2.1$  pF. The 4 pF shown in the diagram is quite conservative, and produces an overdamped response, as shown in the measured response traces of Figure 4x.26.

The second stage is a wideband voltage amplifier, here implemented with a current feedback (CFB) op-amp. The LT1217 maintains 5 MHz bandwidth at  $G = 10$ , with decent accuracy ( $V_{os} = 3$  mV max) and noise ( $e_n = 6.5$  nV/ $\sqrt{\text{Hz}}$ ). The offset trim network is worthwhile, given the 0.5 mV maximum offset of the input stage; you can think of it as a trim of the combined 2-stage offset, if that makes you happier. Both amplifier stages use “high-voltage” op-amps (i.e.,  $\pm 15$  V supplies), permitting output swings to  $\pm 10$  V.<sup>19</sup>

The lowpass filter  $R_5 C_2$  between the stages, with its 300 kHz breakpoint, is important in reducing out-of-band noise. However, as discussed in §8.11.3, we struggle with an ugly current noise whose spectrum rises with frequency. The single lowpass pole introduced at  $f_c$  cancels the rising noise density, but still leaves a noise spectrum flat with frequency (although we do benefit from an additional pole at  $f_{GM}$ ).

#### Sharper lowpass filter.

Better, though, to add a steeper lowpass cutoff to limit the rms noise degradation, which we can do by turning  $U_2$  into a second-order filter, with the addition of two parts, see

<sup>17</sup> It’s unusual to find a case where the bootstrap isn’t a critically important part, the exception being tiny sensors (of the type used for fiber optic receivers).

<sup>18</sup> Sadly *discontinued*! But the CPH3910 from ONSemi is just as good, and available as a dual (CPH3910).

<sup>19</sup> With the photodiode configured to sink current, as shown here, the output will only go positive; but the circuit happily accepts input currents of either polarity.

<sup>16</sup> “That rug really tied the room together . . .”

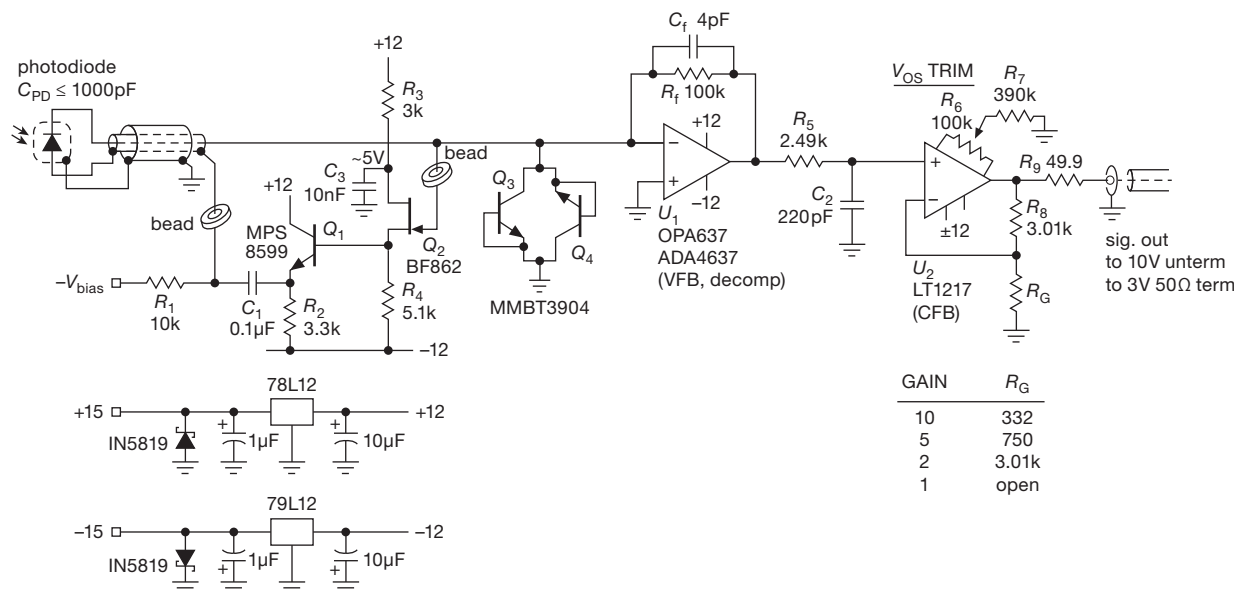


**Figure 4x.25.** A complete photodiode amplifier, suitable for input capacitances up to 1000 pF. Input bootstrapping greatly reduces the effective photodiode and cable capacitance, for enhanced speed and reduced noise.

Figures 4x.27 and 4x.28.<sup>20</sup> The filter's second pole is less effective for gains < 10, where however you're dealing with larger signals, thus less sensitivity to noise filtering. From the response curves (Fig. 4x.28) you might initially choose  $C_1 = 140$  pF for its pretty curve; but sometimes it's nice to exploit a peaky response (e.g., with  $C_1 = 160$  pF) to extend somewhat the response of an amplifier in its rolloff region.

Expensive amplifiers need protection;  $U_1$  will set you back \$30 (!), so we added diode clamps  $Q_3Q_4$  (an *npn* base-collector junction is an inexpensive diode of low capacitance and very low leakage; see for example Figure 5.2).

### 4x.3.5 Gain-switching

The TIA stage in Figure 4x.25 has been set at a fixed gain ( $G = v_{out}/i_{in} = -100$  kΩ), with a selection of higher gain steps provided by the 1–2–5–10× voltage-amplifying stage  $U_2$ . That's OK – but we could do better if instead we increased  $R_f$  to go to higher gain: that's because the (fixed,

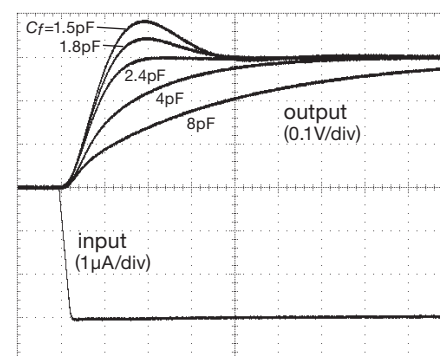


**Figure 4x.26.** Measured response of the transresistance stage ( $U_1$ ) of Figure 4x.25 to a current step input, with an input (summing-junction) capacitance of 100 pF, for several values of feedback capacitor  $C_f$ . Horizontal: 200 ns/div.

100k) low value of  $R_f$  introduces more current noise than the alternative of using higher values of  $R_f$  when we want more gain.<sup>21</sup>

Figure 4x.29 shows two approaches to finessing this problem. We've used the same  $f_T = 80$  MHz op-amp, and we've assumed there's some 25 pF of input capacitance. We should be able to achieve 500 kHz of bandwidth with a gain of 1 MΩ. In circuit A we took the simple solution of a

<sup>20</sup> This is a modification of the VCVS lowpass filter (Fig. 6.28A), in which we've set  $G=10$  and, keeping  $R_1=R_2$ , we've chosen the capacitor values to produce a smooth low- $Q$  roll-off to  $-12$  dB/octave. Put another way, we've broken the rules for a VCVS Butterworth lowpass filter: for  $G=10$  choose  $C_1$  and  $C_2$  to be 0.4 and 2.5 times the respective canonical value of  $C=1/2\pi Rf_c$ . This generalization of the Sallen-and-Key filter was discussed in AoE3's §6.3.2D.

<sup>21</sup> Recall §8.1.1, where resistor current noise is seen to go as  $i_n = \sqrt{4kT/R}$ .

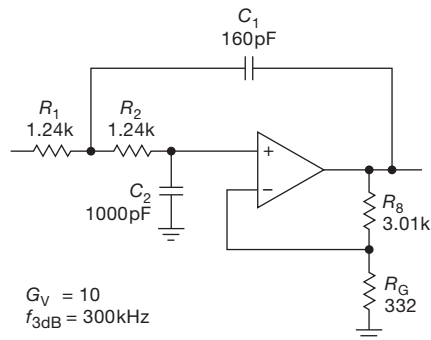


**Figure 4x.27.** Two-pole lowpass filter with  $G=10$  to replace  $U_2$  in Fig. 4x.25.

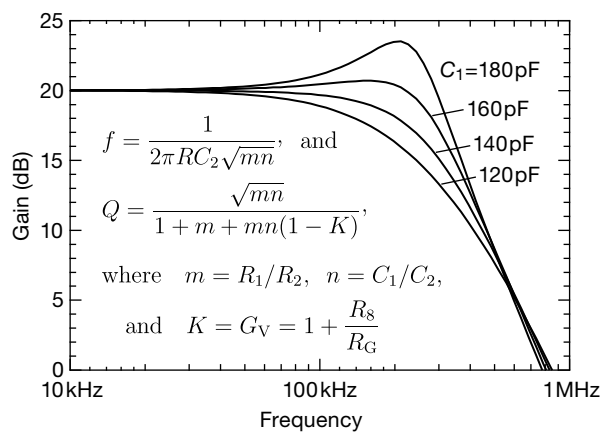


**Figure 4x.28.** Response of the lowpass filter of Fig. 4x.27, as simulated in SPICE. Note the sensitivity to  $C_1$ .

3-position (center-OFF) toggle switch to select the feedback resistor, shunted by appropriate small capacitors, to select TIA gains of 10k, 100k, and 1M. But the problem here is that the switch, in the middle (open) position, introduces some 0.5 pF to 1.5 pF of capacitance that effectively shunts  $R_f$ , overriding the 0.3 pF that's supposed to be across the 1M feedback resistor (there's about 0.1 pF parasitic capacitance of  $R_f$  itself, thus the 0.2 pF explicit capacitor shown). That kills our target 500 kHz bandwidth!<sup>22</sup> We might try replacing the toggle switch with a CMOS SPDT switch; but the parasitic capacitance in the OFF state is even worse than the mechanical switch – about 5 pF.

Circuit B is the better solution: here we've used a CMOS switch, wired “backwards” (in current-steering mode),

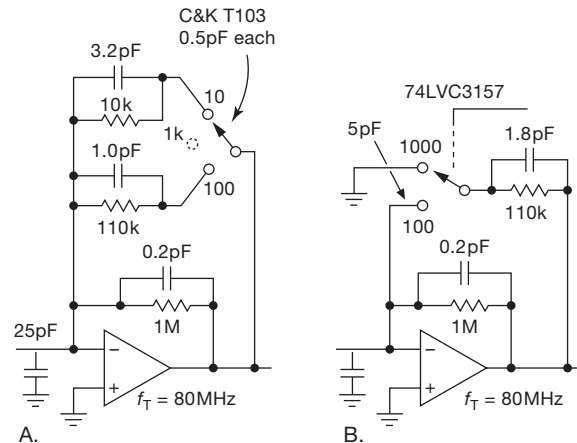


**Figure 4x.29.** Minimizing bandwidth-killing capacitance while gain-switching the TIA with several values of feedback resistor. Circuit B nicely circumvents the degrading effects of parasitic switch capacitance in circuit A.

with the two signal terminals always at ground potential. They switch *currents* (rather than voltages), a scheme we first encountered in Figure 13.47 in Keysight's “Multislope III” converter. The ground potential means we can use a low-voltage switch, even with high-voltage signals. We chose a ‘3157-type switch (see §13.8.5 and Table 13.7) for its low capacitance (accepting its moderately high  $R_{ON}$ ).

In the high-gain position (switch open) we're adding an acceptable 5 pF to the summing junction, while the damaging 100k and 1.8 pF currents are safely shunted to ground. In the low-gain 100k position the switch capacitance increases to 17 pF, forcing us to increase  $C_f$  to 1.8 pF, slightly reducing the bandwidth. The 74LVC1G3157 is available in SOT23-6 and SC70-6 packages, the latter small enough to squeeze in at the summing junction. If you want three gain choices with  $R_f$  switching, you can add a second switch.

#### 4x.3.6 Some loose ends

- Note that you generally can assume that the op-amp is behaving like a classical 6 dB/octave, 90° lagging phase amplifier; you can take a “single dominant pole” model, in engineer's lingo, and you don't have to worry about additional phase shifts that usually creep in as you approach the op-amp's  $f_T$ . That's because the large feedback resistors used in these amplifiers usually put the input pole  $f_{RCin}$  at a very low frequency, such that the trouble region at  $f_{GM} = \sqrt{f_{RCin}f_T}$  is far below the frequencies at which the op-amp departs from the single-pole model.
- For the same reason – namely that the loop gain is

<sup>22</sup> There is a workaround, of sorts, by adding 10 to 20 pF capacitors to ground at each switch terminal – but this is ugly, loading the 80 MHz op-amp, and it's only a partial solution because there's some capacitive signal leaking through, lowering the gain.



brought to unity far below the op-amp's  $f_T$  – you can safely use *decompensated* op-amps in this circuit, as we did with the OPA637 in our second design attempt. That more than doubled the speed, because it has 5 times greater bandwidth ( $f_T = 80\text{MHz}$ ); but it is only stable at closed-loop gains of 5 or greater. A warning, however: if you use decompensated op-amps in this circuit, make sure that the ratio of  $C_{in}$  to  $C_f$  is greater than the minimum specified closed-loop gain (this will usually be true), because that ratio sets the high-frequency closed-loop gain of the transresistance amplifier. Also note that circuit stability depends upon a minimum input capacitance, so the circuit may oscillate with the input unplugged.

- Following similar reasoning, it is possible to raise the gain–bandwidth product inside the feedback loop by cascading two op-amp stages, properly configured. The stability of this arrangement depends on careful placement of the unity-gain crossing of the loop gain within this transresistance configuration – don't try this trick with a conventional *voltage* amplifier!
- We have only briefly discussed here the important issue of *noise* in transresistance amplifiers (which are often called upon to amplify very small signals). That is treated in Chapter 8 of AoE (devoted to low-noise design, including both discrete and op-amp voltage amplifiers), where there's a discussion of the unfortunate property of transresistance amplifiers of converting internal op-amp voltage noise into an effective input current noise, which rises proportional to frequency and to total  $C_{in}$ .
- As in Figure 4x.25, it's good hygiene to put low-capacitance protective clamps at the input of TIAs in which there's risk of high-voltage transients (from a biased detector, etc.). A nice (but unrelated) trick we've seen<sup>23</sup> is the deliberate use of the CMOS op-amp's input protection diodes to reset the integrator capacitor – by simply pulsing the supply rails with a momentary (and current-limited) polarity reversal.
- To trim the compensation it's a good idea to use a test fixture that can provide a clean nanoamp-scale square wave. This is discussed in §8.11.13 in AoE3, with a suggested circuit (Fig. 8.91).

#### 4x.3.7 Designs by the masters: A wide-range linear transimpedance amplifier

The dynamic range (i.e., ratio of maximum to minimum input current) of a resistance-feedback transimpedance amplifier like that in Figure 4x.16A is limited by several fac-

tors. First, the op-amp's input bias current sets an approximate lower bound on measurable currents, typically somewhere around a picoamp for op-amps of reasonable precision (but as low as 10 fA for less accurate CMOS parts<sup>24</sup>).

Second, for a given feedback resistance  $R_f$ , the current range is bounded at the high end by the op-amp's supply voltage, i.e.,  $I_{\max} \leq V_S/R_f$ ; and at the low end it becomes inaccurate when the output approaches the op-amp's offset voltage, i.e.,  $I_{\min} \geq V_{os}/R_f$ . These constraints limit the dynamic range to  $I_{\max}/I_{\min} \lesssim V_S/V_{os}$ . In practical terms, that's roughly a dynamic range of  $10^5$  ( $\sim 10\text{V}/100\mu\text{V}$ ) for low-offset op-amps.

One way to get a larger dynamic range is to use nonlinear diode-like feedback to create a logarithmic response (see §4x.20). For some applications this is just what you want. But this method suffers from several drawbacks: (a) you can't average or lowpass-filter the output voltage to get the average input current (because the average of the log is not the log of the average); (b) it's difficult to get significant precision, say at the part-per-thousand level, owing to drift and calibration uncertainties; and (c) you often want good linearity with signals of both polarities (and which cross through zero).

What you want, then, is a linear precision TIA that somehow spans multiple sensitivity ranges simultaneously. Figure 4x.30 shows an elegant implementation, devised by Stephen Eckel and his team at Yale University.<sup>25</sup> The basic topology is a standard resistive-feedback TIA, here implemented with op-amp  $A_1$  and a series string of resistors ( $R_1 - R_3$ , with successive ratios of 100:1) that individually would span four decades of full-scale sensitivity. To this basic circuit JFETs  $Q_1 - Q_4$  have been added, which go into conduction progressively as each range reaches full-scale output; this prevents op-amp  $A_1$  from saturating, as explained below.

Here's how it works: for the lowest input currents ( $I_0 < 100\text{nA}$ ) the voltage developed at  $A_1$ 's output is just  $I_0(R_1 + R_2 + R_3)$ , and output amplifier  $A_2$ 's gain (approximately  $\times 2$ ) is chosen to produce 10 V output (called  $V_1$ ) for 100 nA input. That input current is full-scale for the most sensitive range, and at that current the op-amp's output is approximately 5 V. The other output amplifiers  $A_3$

<sup>24</sup> With the stunning exception of the ADA4530-1, with its 1 fA typ (20 fA max) bias current at 25°C, remarkably combined with a precise  $9\mu\text{V}$  typ ( $50\mu\text{V}$  max) offset voltage. Its noise performance is, uh, underwhelming – some  $80\text{nV}/\sqrt{\text{Hz}}$  at 10 Hz.

<sup>25</sup> S. Eckel, A.O. Sushkov, and S.K. Lamoreaux, "A high dynamic range, linear response transimpedance amplifier," *Rev. Sci. Instrum.*, **83**, 026106 (2012).

<sup>23</sup> Thanks to Bernie Gottschalk for this elegant suggestion.

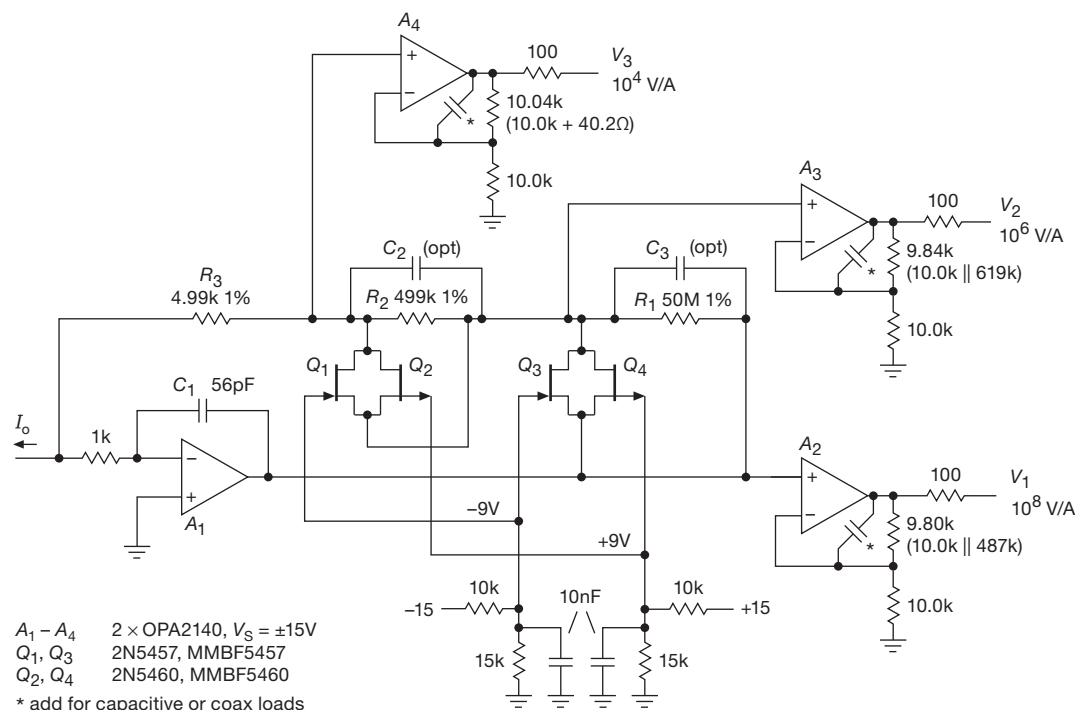


**Figure 4x.30.** Wide dynamic-range linear transimpedance amplifier, with three simultaneous outputs with sensitivities in ratios of 100:1. The JFETs  $Q_1$ – $Q_4$  shunt current around each gain-setting feedback resistor after the respective stage passes its full-scale output.

and  $A_4$  generate the outputs for the higher-current ranges:  $A_3$  picks off the voltage developed by  $I_0$  flowing through  $R_2 + R_3$ , and  $A_4$  picks off the voltage developed by  $I_0$  flowing through  $R_3$  alone.

Now for the trick: for input currents significantly greater than 100 nA,  $A_1$ 's output would saturate, but that is prevented by  $Q_3$  or  $Q_4$ . For example, an input sinking current of 200 nA, which would bring  $A_1$ 's output to +10 V, instead causes  $p$ -channel JFET  $Q_4$  to conduct (its gate is biased at +9 V), effectively shunting  $R_1$  and preventing saturation. So the TIA loop remains in the active region, and  $A_3$ 's output ( $V_2$ , with its sensitivity of 1 V/ $\mu\text{A}$ ) will be at the correct +0.1 V. Similarly, input currents great enough to bring  $V_2$  beyond full-scale cause  $Q_2$  to shunt current around  $R_2$ , again preventing  $A_1$ 's saturation.

Figure 4x.31 shows measured performance, plotted on log–log axes, illustrating nicely the stacking of simultaneous linear outputs, each of which saturates just beyond full-scale. These data were taken for positive output polarity only (i.e., input sinking current, shown as  $I_0$  in the circuit diagram), but the circuit as drawn works properly for both polarities, notionally illustrated (on linear axes) in Figure 4x.32 and seen accurately in the measured data of

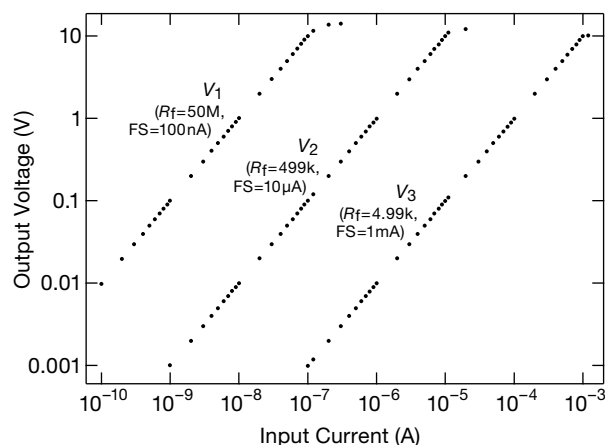


**Figure 4x.31.** Measured simultaneous outputs of the wide-range transimpedance amplifier of Figure 4x.30, demonstrating a dynamic range of  $10^7$ :1. For  $V_2$  and  $V_3$ , corrections (i.e., zero-current offsets) of 0.12 mV and 0.045 mV were applied; they barely nudged the lowest few points.

Figure 4x.33. If only one polarity is required, the complementary JFETs in Figure 4x.30 can be omitted.

A few comments on the circuit: (a)  $C_1$  provides fre-

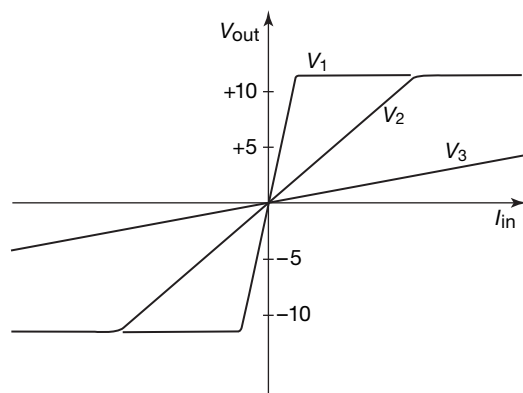


**Figure 4x.32.** The wide-range TIA, implemented with split supplies and with JFETs of both polarities (Fig. 4x.30), generates simultaneous linear outputs that transition smoothly through zero, as indicated in this sketch (with gain ratios of 5:1) and in the measured data in the next figure.

quency compensation; the 56 pF value we used would need to be increased for a capacitive input source.

(b) Additional compensation capacitors  $C_2$  and  $C_3$  can be used to tailor frequency response of the individual ranges; we omitted them for our measurements.

(c) The series 1k input resistor protects  $A_1$  if the input is overdriven; it has no effect on performance.

(d) We chose OPA2140 op-amps for their low  $V_{OS}$ , low  $I_B$ , and good value (see the mini-table below); the low-current performance could be improved somewhat with OPA627B’s (expensive), or considerably more with the ADA4530-1 (but with poorer noise performance).

(e) To obtain the full dynamic range, it’s necessary that the leakage currents of JFETs  $Q_1$ – $Q_4$  be no more than a few picoamps. The guidance provided by the datasheets will leave you sleepless: worst-case gate reverse currents of 1000 pA and 5000 pA (for  $n$ - and  $p$ -channel, respectively, at room temperature and 15 V–20 V reverse bias). And, if you worry about *channel* leakage when cutoff, the datasheet is particularly unhelpful, specifying only a range of gate voltages to produce “cutoff” drain currents of 10,000 pA and 1,000,000 pA (for  $n$  and  $p$  types, respectively). Happily, the manufacturers are highly conservative, and the actual situation is far better: we measured total leakage currents (at room temperature, and at gate-to-drain voltages to 15 V) ranging from 0.1 pA to 3 pA for 17 JFET samples; see the discussion in §2x.1.

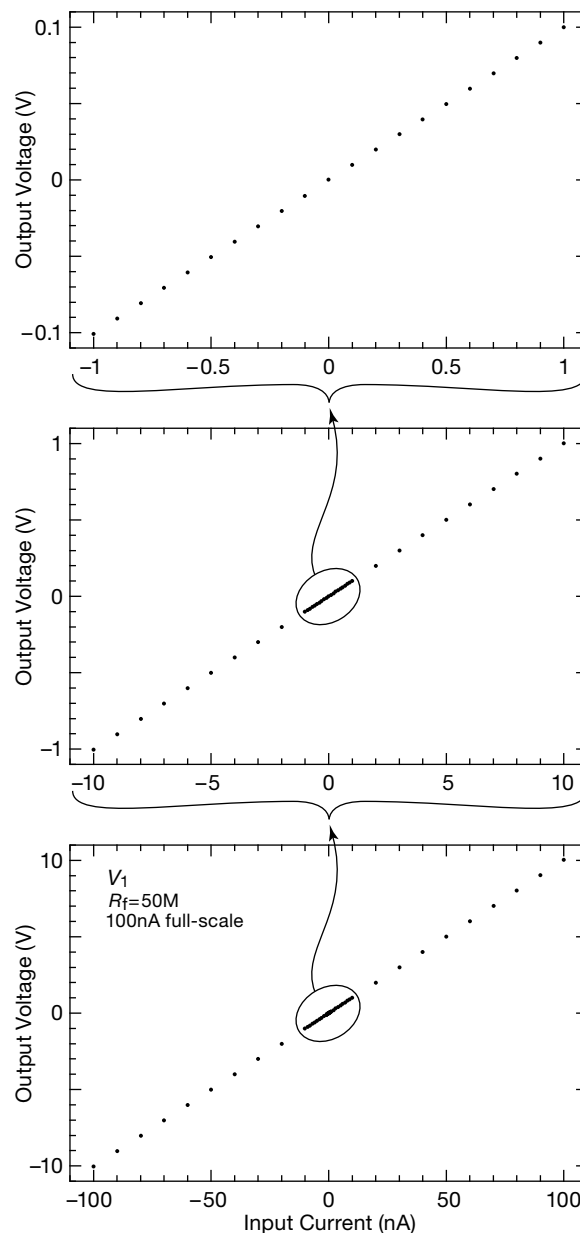


**Figure 4x.33.** These linear plots of output voltage versus input current for the most sensitive scale (i.e.,  $V_1$ : 0.1V/nA) show the TIA’s linearity straight through zero input current. No corrections have been applied to these measured data.

### 4x.3.8 A “starlight-to-sunlight” linear photometer

Here’s a nice application for a wide-range linear transimpedance amplifier of the kind described in §4x.3.7 (which you should read first): a photometer that measures

Type <sup>a</sup>	V <sub>os</sub>		I <sub>b</sub>		e <sub>n</sub>		i <sub>n</sub>	Price qty 10 (US\$)
	typ	max	typ	max	10Hz	1kHz		
	(μV)	(μV)	(pA)	(pA)	(nV/√)	(nV/√)	(fA/√)	
OPA627B	40	100	1	5	15	5.2	1.6	30.81
OPA2140 <sup>b</sup>	30	120	0.5	10	8	5.1	0.8	5.38
ADA4530-1 <sup>c</sup>	9	50	0.001	0.02	80	16	0.07	21.72

Notes: √ = nV/√Hz. (a) except as noted, V<sub>S</sub>=36V max total supply.  
(b) dual. (c) V<sub>S</sub>=16V max total.

**Figure 4x.34.** Op-amp choices for wide-range linear transimpedance amplifier.

a wide range of illumination,<sup>26</sup> going from sunlight to starlight. This really pushes the limits of dynamic range, ranging over some 8 orders of magnitude: bright sunlight is approximately 110,000 lux, and dark-sky starlight is about 0.002 lux (100 times darker than the full moon’s 0.25 lux). And we’d really like 9 orders of magnitude, to give us 10% accuracy at the lowest light levels.

Because the photocurrent is unipolarity, we can run the circuit from a single supply polarity (almost – see discussion below). We also need only p-channel JFETs for the successive resistor clamping circuits. We chose the transimpedance gains of the taps in the ratio 300:1 ( $R_1$ ,  $R_2$ ,  $R_3$ ), with full-scale output of +5 V; the output voltages are digitized by a 3-channel, 12-bit ADC running from +5 V and ground. The TIA stage is powered from +12 V, to accommodate the over-range behavior of the wide-range TIA scheme, while the unity-gain buffers and the ADC run from +5 V; the 10k resistors  $R_4$ – $R_6$  limit current into the input clamp diodes to less than 1 mA. Figures 4x.36 and 4x.37 show SPICE simulations of the input-current to output-voltage transfer characteristics: the log–log plot is helpful for seeing the stacked linear outputs, and the log–linear plot illustrates nicely the successive clamping as each stage saturates.

A significant challenge in this design was the choice of op-amps. The input (TIA) stage  $A_1$  must run at 10–12 V to preserve a 5 V full-scale output on each tap (illustrated graphically in the plots of Fig. 4x.37), but we need more: its input current must be down in the 0.5LSB range (i.e., <6 pA), and its offset voltage should be less than the

voltage step corresponding to 0.5LSB of the ADC (i.e., <0.6 mV). It also must operate with the inputs at ground, and its output voltage range must extend to ground (RRO). For the buffer op-amps  $A_3$  and  $A_4$  we can use a low-voltage part (i.e., +5 V single supply), but with rail-to-rail input and output.

With these constraints we found two good candidates for  $A_1$  – TI’s LMP7701 and LTC’s LTC6240HV – and two candidate dual op-amps for  $A_3A_4$  – ADI’s AD8616 and LTC’s LTC6078. The table lists their relevant specifications. For the input stage  $A_1$  we’re down around 0.2LSB for  $V_{os}$  and 0.1 LSB for  $I_B$ , conservatively taking the worst-case (max) values. But these are FET inputs, so we should expect significantly higher bias currents at elevated temperatures; even so, we’re OK up to 60°C or so. For the followers  $A_3A_4$  the dual op-amps AD8616 and LTC6078 meet our requirements.

The photodiode was chosen to match the amplifier’s gain and dynamic range. The S1133-14 is an inexpensive silicon photodiode in a ceramic package, producing 3 mA in full sunlight; it’s being operated here in photovoltaic mode (zero bias), but it does see the op-amp’s offset voltage across its terminals. No worry, though – the S1133-14 photodiode spec shows dark current (with an extravagant 10 mV bias) as 0.2 pA (typ), and sloping down to an extrapolated current less than 0.1 pA at 1 mV bias. The S2387-33R photodiode does even better, in fact specifying a maximum leakage of 5 pA at 10 mV bias (and a typical value of 0.1 pA).

### “Getting to ground”

And now for the troublesome business of RRO op-amps not delivering on their promise: the cruel fact is that most RRO op-amps operating with a single positive supply cannot bring their output fully to ground, even when unloaded. The  $V_{OL}$  specs in the table (taken from the datasheets) show this problem, which we discuss in further detail in §§4x.11.3 and 4x.11.4; but, put simply, the quiescent current through the op-amp’s push–pull output stage produces a drop across the pulldown transistor’s  $R_{ON}$ . In §4x.11.4 we show two ways of dealing with this (sinking current from the op-amp’s output, or bringing the op-amp’s negative supply terminal a hundred millivolts or so below ground). We prefer the latter, and we’ve indicated such a connection on the schematic.

Some additional circuit details: (a) Because full-scale current for the least-sensitive range is 5 mA (compared with 1 mA for the circuit of Fig. 4x.30), we chose a larger JFET (type J175), which specifies  $I_{DSS}$ =7 mA (min). You may worry about JFET leakage current compromising the

<sup>26</sup> Officially, *illuminance*, which is the flux of light per unit area (lumens/meter) upon a surface, weighted to take account of the eye’s spectral sensitivity. Photometric units can drive you nuts, with candela, lumen, lux, and a host of confusing names like radiant flux, radiant intensity, radiance, irradiance, radiosity, radiant exitance, radiant exposure, luminous flux, luminous intensity, luminance, illuminance; and most of these can host the modifier “spectral,” meaning the same photometric quantity per unit frequency (or per unit wavelength). See also §9x.22.

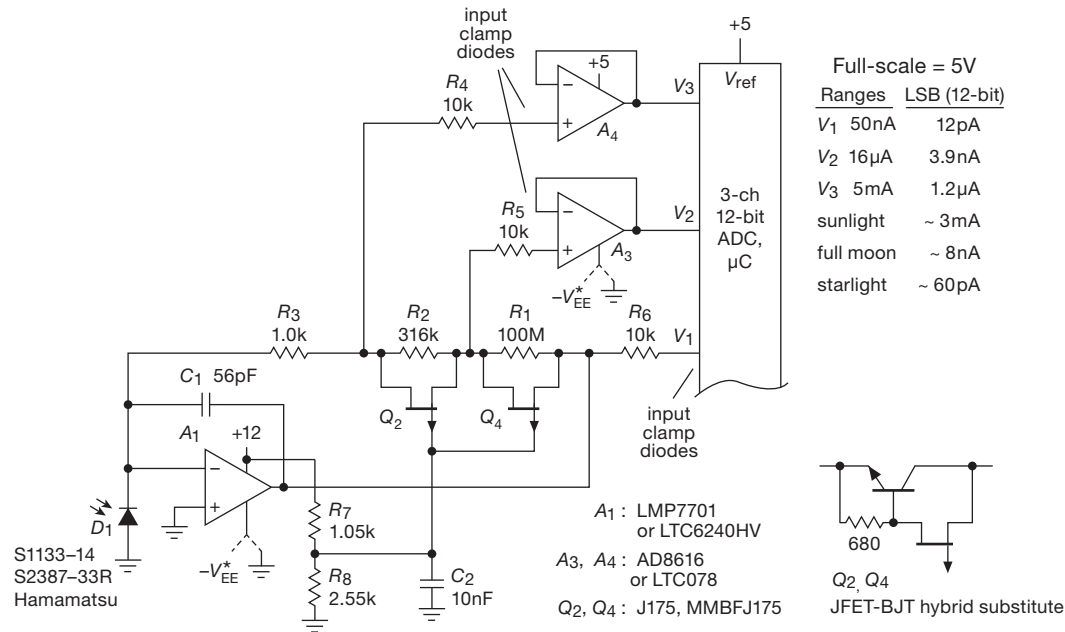


**Figure 4x.35.** Starlight-to-sunlight linear photometer, based on the method of §4x.3.7. The  $V_{SS}$  terminal of the “single-supply” op-amps should be powered from  $-100\text{ mV}$  or so, to ensure operation all the way to ground; see §4x.11.3.

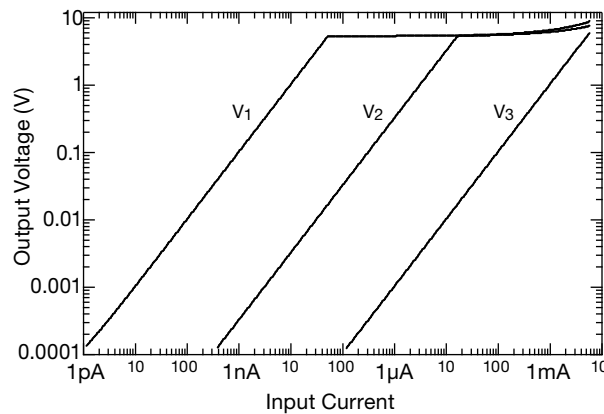


**Figure 4x.36.** SPICE simulation of the three output voltages versus (sinking) input current, for the circuit of Fig. 4x.35.

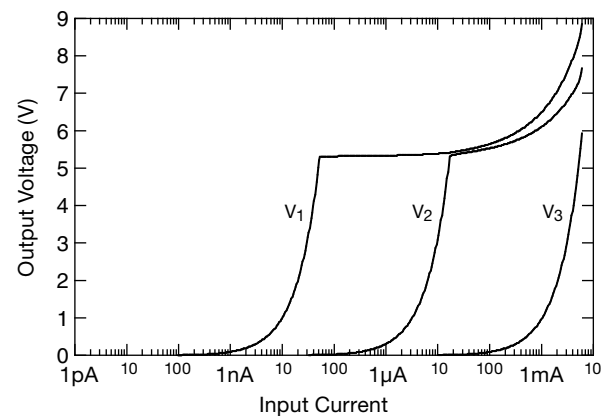


**Figure 4x.37.** Same data as Fig. 4x.36, plotted on log-linear scales.

dynamic range at the low-current end; but, in spite of its larger die geometry, the several samples we measured<sup>27</sup> exhibited leakage currents of only 1 pA at room temperature (with as much as 15 V gate-to-channel bias).

(b) Another way to extend the operating current is to add a small *npn* BJT to  $Q_2$  and  $Q_4$  as shown in the inset in Figure 4x.35. If you go this route, be warned that BJT leakage

is highly unpredictable, as we found by actual measurement, see §2x.1.

(c) The loose  $V_P$  specification makes it difficult to set  $Q_2$ 's and  $Q_4$ 's gate bias: 3 V (min), 6 V (max). We've complained about this JFET ugliness before, you know the drill. It's probably best to trim the bias manually (and while you're at it, measure the output with zero input current, to ensure that leakage effects do not prevent proper operation down to  $\sim 10\text{ pA}$  or so).

<sup>27</sup> See the discussion of transistor leakage in §2x.1.



Type	V <sub>supply</sub> (V)	I <sub>b</sub> <sup>a</sup>		V <sub>os</sub>		V <sub>oL</sub>		I <sub>s</sub> typ (mA)	GBW typ (MHz)
		typ	max	typ	max	typ	max		
LMP7701	2.7-12	0.2 <sup>b</sup>	1 <sup>b</sup>	37	200	40 <sup>c</sup>	50 <sup>c</sup>	0.8	2.5
LTC6240HV	2.8-11	0.5 <sup>b</sup>	1 <sup>b</sup>	60	250	15	30	2.7	18
AD8616 <sup>d</sup>	2.7-5.5	0.2	1	80	500	7.5 <sup>e</sup>	15 <sup>e</sup>	1.7 <sup>f</sup>	24
LTC6078 <sup>d</sup>	2.7-5.5	0.2	1	25	100	1	–	0.06 <sup>f</sup>	0.75

Notes: (a) at T=25°C. (b) at V<sub>S</sub>=+10V. (c) when sinking 0.5mA. (d) dual. (e) when sinking 1mA. (f) per amplifier.

Figure 4x.38. Op-amp choices for Fig. 4x.35.

4x.3.9 Autoranging wideband transimpedance amplifier

In §4x.3.7 we presented a linear TIA with a seven-decade dynamic range. The trick was to generate three simultaneous linear outputs, each with its own gain factor (going by factors of 100); so the output with the highest gain pins at full scale, while the others continue working. The input current is then read from the most sensitive non-saturated range. We used this same trick in §4x.3.8 to create a “starlight-to-sunlight photometer” with linear outputs and with sensitivity to photocurrents from 1 pA to 5 mA (a factor of 5 × 10<sup>9</sup>).

As nice as those circuits are, they do have the drawback of rather limited bandwidth. For example, in Figure 4x.30 the “bypass” JFETs Q<sub>3</sub> and Q<sub>4</sub> add bandwidth-robbing capacitance to ground at the downstream side of the highest-value (50MΩ) feedback resistor R<sub>1</sub>. Ordinary (single-gain) transimpedance amplifiers, lacking bypass JFETs, do not suffer from this problem.

But there’s another way to achieve wide dynamic range in a linear transimpedance amplifier, based on a suggestion by the ever-creative John Larkin. Look at Figure 4x.39, which illustrates this novel technique in the context of a wideband photodiode amplifier (where we’ve chosen OSI’s PIN-13D silicon photodiode: 13 mm<sup>2</sup> area in a TO-5 hermetic package).

In this unusual circuit the lower-sensitivity ranges start operating after each more-sensitive range saturates, and (unlike the earlier schemes) the input current is derived as a weighted sum of the outputs of all the individual gain stages, as we’ll see presently.

In this single-polarity circuit, TIA amplifier A<sub>1</sub> (a wideband RRIO with 3 pA bias current) operates normally until enough input current causes its output to saturate at the positive supply rail. Further input current causes A<sub>1</sub> to lose control of its summing-junction node, whereupon the voltage at its inverting input drops below ground enough to

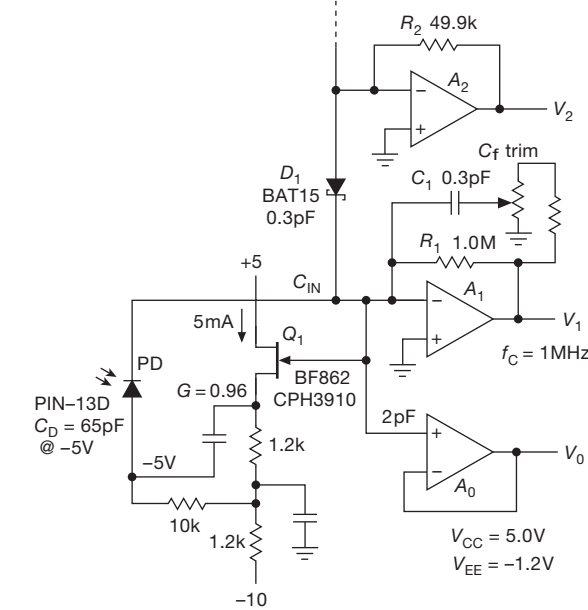


Figure 4x.39. Linear autoranging TIA. When high-gain TIA A<sub>1</sub> saturates, lower-gain A<sub>2</sub> absorbs the additional input current, while A<sub>0</sub> corrects for the offset at A<sub>1</sub>’s summing junction.

forward bias Schottky diode D<sub>1</sub>, allowing amplifier A<sub>2</sub> to take over.<sup>28</sup> The use of rail-to-rail op-amps allows us to know the saturation voltage, thus the current through the feedback resistor when stage A<sub>1</sub> (and subsequent stages, if used) is in saturation.

Once A<sub>2</sub> takes over, A<sub>1</sub>’s summing junction (buffered by A<sub>0</sub>) will be below ground by a Schottky diode drop, which means the current through R<sub>1</sub> is now (V<sub>1</sub> – V<sub>0</sub>)/R<sub>1</sub>, so the correct input current (sinking) is just

$$I_{in} = \frac{V_1 - V_0}{R_1} + \frac{V_2}{R_2}$$

(4x.3)

Bandwidth

It’s a struggle to get bandwidth in a high-gain TIA. To achieve 1 MHz in a TIA with 1MΩ feedback resistance we needed a feedback capacitance C<sub>f</sub> of 0.16 pF, implemented here with a 0.3 pF capacitor “tuned” with a trimmer.

The total capacitance at the summing-junction node C<sub>in</sub> is the sum of Q<sub>1</sub>’s feedback capacitance C<sub>rss</sub>, plus the common-mode and differential capacitances of A<sub>0</sub> and A<sub>1</sub>, plus D<sub>1</sub>’s capacitance at zero bias, plus the (bootstrapped) capacitance of the photodiode.<sup>29</sup> The latter is a bit less than 5% of the photodiode’s 65 pF capacitance at –5 V, thanks

<sup>28</sup> The photodiode’s bias will drop slightly, but this is of no consequence.  
<sup>29</sup> See §8.11.9.

to the bootstrap from JFET follower  $Q_1$  (whose voltage gain is  $>0.95$ ). These terms add up to about 11.2 pF, for an  $f_{RC}$  of 14.2 kHz – the penalty over a conventional single-gain TIA is only 2.3 pF, great!. With the 100 MHz rail-to-rail OPA357 for  $A_1$  and a CPH3910<sup>30</sup> for  $Q_1$ , we get an  $f_{GM}$  of 1.2 MHz, and the damping factor for  $f_c = 1.0$  MHz is about 0.8 (see §4x.3.2). Overall we're getting a bandwidth improvement (for equivalent transimpedance gain) of some  $10\times$ – $20\times$ , as compared with the JFET-bypass scheme of §4x.3.8.

### Some details.

(1) For  $D_1$  we chose a small-die Schottky diode, BAT15-03W, for its low 0.3 pF capacitance. At 100  $\mu$ A (where  $A_2$  goes into saturation) the diode's drop is about 180 mV, which adds about 4% current through  $R_1$ ; that is why follower  $A_0$  is needed to get 1% precision in this circuit.

(2) Because the summing junction is pulled a diode drop below ground when  $A_1$  saturates, it's necessary<sup>31</sup> to power its negative rail a volt or so below ground; here we chose  $-1.2$  V (two diode drops, easily generated).

(3) We're powering our op-amps with a precision  $+5.0$  V supply. The OPA357 has a 7.5 V absolute maximum rating, enough for us to use more than a  $-1.2$  V negative rail. If you wanted a higher saturated output voltage (say  $+10.0$  V), this would be a good place to use a composite amplifier configuration (see Figure 8.78 for inspiration).

(4) This scheme can be extended to additional stages, by adding another Schottky diode and (lower gain) TIA stages at the top. Each stage (except the topmost) needs a follower to track its summing-junction offset at saturation; and each stage increases the negative offset of lower stages by a diode drop. So it may be better to use the “JFET-bypass” method (Figure 4x.35) for the lower-gain stages, where higher capacitances wouldn't matter. But in the example here,  $A_1$  is the special high-gain stage where it's hard to achieve a 1 MHz bandwidth in a TIA stage with 1 M $\Omega$  feedback resistance.

### 4x.3.10 Multiple-range cascode-bootstrap wideband TIA

Continuing the theme of wideband transimpedance amplifiers, the critical bandwidth-robbing (and  $e_nC$  noise-degrading) issue of summing-junction capacitance in photodiode amplifiers can be nicely addressed by a combination of an isolating cascode transistor and a bootstrap of the low side of the photodiode. We've seen these before

(JFET bootstrap: Figure 4x.39 and §8.11.9; and cascode with bootstrap: §8.11.10), but not in the context of gain-switching.

Here we combine these bandwidth-enhancing techniques with the ability to switch the transimpedance gain. Figure 4x.29 showed the best way to connect an SPDT switch to change the gain of a wideband TIA, but it did not include circuitry to reduce summing-junction capacitance, which is almost always needed in a wideband TIA.

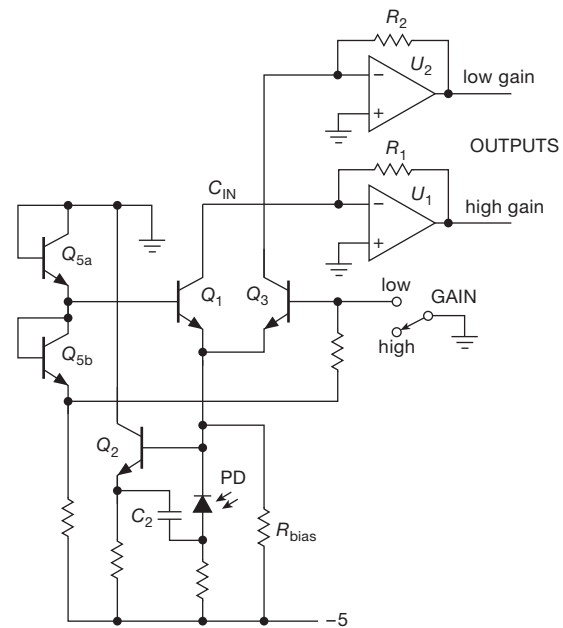


**Figure 4x.40.** Cascode-bootstrap wideband transimpedance amplifier with multiple switch-selected gain outputs.

Figure 4x.40, based on suggestions by Phil Hobbs,<sup>32</sup> fills this gap. In this circuit  $Q_2$  is the bootstrap follower that dramatically lowers the effective photodiode capacitance, which is then isolated from the summing junction by cascode transistor  $Q_1$ . This enables both greater bandwidth and lower  $e_nC$  noise.

Before explaining the gain-switching, some important comments on the circuit so far:

(1)  $Q_2$ 's operating current must be somewhat higher than the maximum photodiode current, making its base current

<sup>30</sup> To replace the popular BF862, inexplicably discontinued by NXP.

<sup>31</sup> But see §4x.11.3.

<sup>32</sup> For a good first reading assignment, try his “Photodiode Front Ends – The REAL Story,” *Optics and Photonics News*, April 2001, pp 42–45. And follow that with his book *Building Electro-Optical Systems, Making It All Work*, 2nd ed., Wiley (2009), a fine collection of tricks for designing cascode photodiode amplifiers, including series peaking inductors and  $T$ -coils to extend the bandwidth, noise cancellers, and more.

a possible issue at low photodiode currents. Hobbs suggests using a high-beta MPSA18 (similar to 2N5089); the MMBT6429 and MMBT5962 are candidate surface-mount alternatives.

(2) The photodiode capacitance  $C_{PD}$  is in parallel with  $Q_1$ 's base-emitter capacitance  $C_\pi$  (see §2x.1.1). This lowers  $Q_1$ 's effective  $f_T$ , which we want to keep well above  $f_c$ . For example, a 2N5089 has an  $f_T$  of about 2 MHz at 10  $\mu\text{A}$  (see Figure 2x.80 and note how  $f_T$  increases roughly proportional to  $I_C$  at low currents, due to fixed  $C_\pi = C_{je}$  values below 30  $\mu\text{A}$ ). To make the cascode work at low photodiode currents we exploit  $Q_2$ 's bootstrapping to reduce  $C_{PD}$  to values well below  $C_\pi$  of  $Q_1$ . We may also need to add  $R_{bias}$  to maintain a minimum current through  $Q_1$  (Hobbs added 8  $\mu\text{A}$ ).<sup>33</sup>

Now for the gain-switching: We start by adding dual transistor<sup>34</sup>  $Q_5$  to generate two stacked voltages just below ground, and we use the first voltage to bias our primary cascode transistor  $Q_1$ . Generally you'd dedicate  $Q_1$  to the highest-gain stage. The second lower voltage is used to back-bias the unused secondary cascode-transistor candidates  $Q_3$ ,  $Q_4$ , etc. These transistors can be turned on individually to take over the photodiode current, by switching their base to ground.<sup>35</sup> This scheme can be extended to additional range stages, each with its separate output. Unlike the two autoranging approaches discussed earlier, in this scheme you must select the single active range and output. However, you could use one of the cascode transistors to feed a JFET-bypass or diode-stacked autoranging circuit, as described in §§4x.3.7, 4x.3.8, and 4x.3.9.

<sup>33</sup> You can cancel most of this extra current with resistors from the summing junction to the positive supply, for example as shown in Fig. 8.87. But if you do that in the gain-switched circuit here (Fig. 4x.40), the “off” op-amp will saturate at the negative rail). These considerations reduce the attractiveness of this circuit for photocurrents below 100 nA.

<sup>34</sup> Some dual *npn* transistor choices are the DMMT3904W or MMDT3904. We like Diodes Inc.'s selection of dual transistors in SOT-23-6 (SOT-26) or SC-70-6 (SOT-363) and smaller(!) packages.

<sup>35</sup> Increasing the photodiode's back-bias by half a volt, of no consequence.